# Halogen adsorption on transition-metal surfaces: A case study of Cl on Ta(110)

Christine J. Wu and John E. Klepeis
*Lawrence Livermore National Laboratory, University of California, Livermore, California 94551*
(Received 6 December 1996)

Through a series of *ab initio* calculations, we not only predict the atomic and electronic structure of Cl on Ta(110), but also provide a quantitative basis for understanding a number of controversial questions regarding halogen adsorption on transition-metal surfaces. We demonstrate that a simple dipole layer model accurately describes the unexpected decrease in the work function upon halogen absorption, and that our proposed overlayer structure explains the one-dimensional streaking in the low-energy electron-diffraction pattern of the adsorbate-covered surface. An analysis of the electronic structure suggests that transition metals such as Ta look like simple metals from the point of view of highly electronegative adsorbates such as Cl. [S0163-1829(97)07915-0]

## I. INTRODUCTION

Relative to the large number of studies of halogen adsorption on semiconductor surfaces,[1] the amount of information available for transition-metal surfaces is considerably lacking, particularly at the atomic scale. In addition, there has been much speculation regarding the nature of the halogen–transition–metal chemisorption bond. Lastly, Cl is a potential etching reagent for Ta thin films used in inkjet printer technology. Our interest in the Cl-covered Ta(110) surface is therefore driven partly by its technological importance but also to initiate a general, atomic-level understanding of halogen adsorption on transition metals. In particular, the Cl/Ta(110) system exhibits two controversial phenomena which are common to a number of bcc transition-metal (110) surfaces upon halogen adsorption: (1) the work function decreases unexpectedly[2–7] and (2) the low-energy electron-diffraction (LEED) pattern exhibits one-dimensional streaking.[8–10] Several empirical models[2,4,6,8] have been proposed, but none has attempted to explain both phenomena within a single coherent framework. Furthermore, the accuracy of these models has not been tested because the local atomic and electronic structure was not known.

All previously reported studies for Cl overlayers on Ta have been experimental in nature. Stott and Hughes[7] found that the work function increases upon Cl adsorption for Ta(100), as expected based on the relative Ta and Cl electronegativities, but that it decreases for Ta(110). With the exception of F, similar decreases for other halogens have been observed on the (110) surfaces of different bcc metals, including W (Refs. 2–5) and Cr.[6] A number of explanations for the observed work-function decreases have been proposed: (1) penetration of the halogen atoms below the surface, thereby creating a dipole layer of the opposite sign,[2,6] (2) a complex adsorption process involving both atomic and molecular adsorbate phases,[2] and (3) covalent bonding combined with a simple dipole layer model.[4] Among them, Cl subsurface penetration is the most commonly invoked mechanism[11] for the formation of a positive adsorbate-induced dipole. However, this mechanism fails to explain the work-function increase for both (100) surfaces and F adsorption, where halogen subsurface penetration should be enhanced due either to the more open surface or the smaller adatom.

The observed one-dimensional streaking complicates the interpretation of the LEED data, thus making it difficult to determine the morphology of the Cl overlayer on Ta(110). It is unclear whether the streaking, observed along the $[\bar{1}10]$ direction,[9,10] is caused by reconstruction of the substrate or the structure of the overlayer itself. This phenomenon has been reported for other systems, including S on Mo(110), where Peralta, Berthier, and Oudar[8] attributed it to the formation of vacancy rows. However, no physical driving force has been found for creating vacancy rows, except as a means for reproducing the observed LEED pattern. Nonetheless, this model was also used to explain the data for Cl on Ta(110).[7,10]

In this paper, we present an *ab initio* study of the adsorbate-substrate and adsorbate-adsorbate interactions for Cl on the Ta(110) surface. The resulting detailed, atomic-scale information enables us to predict the minimum-energy structure for a Cl overlayer at various coverages, and to give quantitative explanations for all of the observed phenomena.

## II. CALCULATIONAL DETAILS

Our *ab initio* total-energy calculations are based on density-functional theory and the local-density approximation.[12] We have used norm-conserving Ta and Cl pseudopotentials[13,14] to treat the valence-core electronic interactions. The wave functions were expanded in a plane-wave basis set up to a cutoff of 40 Ry, which gives absolute total-energy convergence to within 0.05 eV for an isolated Cl atom. We have adopted the same exchange-correlation functional,[15] **k**-point sampling[16] ($4\times4\times2$), basis set cutoff (40 Ry), theoretical lattice constant ($a_0 = 3.22$ Å), and seven-layer Ta(110) supercell as in our previous work on clean Ta(110).[14] Cl atoms were placed symmetrically on both surfaces of the supercell. A vacuum region of 17 Å was introduced to separate the slabs.

The Cl adsorption energy $E_{ad}$ was calculated directly from the *ab initio* total energies,

$$E_{ad} = E_{Ta\text{-}Cl} - E_{Ta} - E_{Cl},$$

 © 1997 The American Physical Society

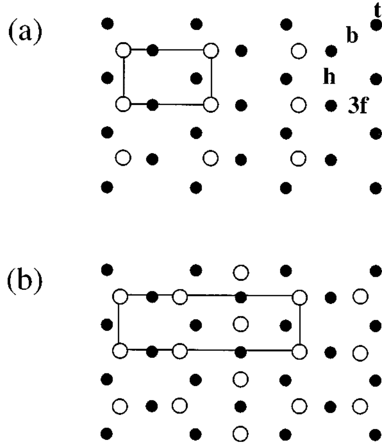


FIG. 1. Schematic diagram of the predicted optimal structures for coverages of (a) 0.5 ML and (b) the saturation coverage of 0.75 ML. The empty and filled circles indicate the positions of Cl and surface Ta atoms, while the letters *t*, *b*, *h*, and 3*f* in (a) represent the positions of the top, bridge, hollow and threefold sites.

where $E_{\mathrm{Ta}}$ and $E_{\mathrm{Ta\text{-}Cl}}$ are the total energies per surface atom of the clean and Cl-covered surfaces, and $E_{\mathrm{Cl}}$ is the total energy of an isolated Cl atom. As a means for understanding the coverage dependence of the adsorption energy, we write $E_{\mathrm{ad}}$ as the sum of two interaction energies:

$$E_{\mathrm{ad}}=E_{\mathrm{bond}}+E_{\mathrm{rep}}.$$

We define the attractive Ta-Cl bonding term $E_{\mathrm{bond}}$ to be independent of the Cl-Cl nearest-neighbor distance, and thus a constant as a function of Cl coverage. With this definition all of the coverage dependence is contained in the repulsive Cl-Cl interaction $E_{\mathrm{rep}}$, but both terms will depend on the adsorption geometry. Our *ab initio* results demonstrate that these definitions lead to an accurate, atomic-scale framework for understanding the Cl adsorption energetics. We have considered four different high-symmetry adsorption geometries on Ta(110): the top, bridge, hollow, and threefold sites which are illustrated in Fig. 1(a).

## III. RESULTS

### A. Cl-Cl repulsion

We expect the Cl-Cl mutual repulsion $E_{\mathrm{rep}}$ to depend strongly on the Cl-Cl nearest-neighbor distance when it is smaller than some threshold value $R_T$. In order to determine $R_T$ we have carried out total-energy calculations for coverages ranging from 1/8 to 1 ML. A coverage of 1/8 ML corresponds to eight atoms per surface layer. Computational limitations preclude the use of a nine-layer (7 Ta+2 Cl) supercell for 1/8 ML, and therefore, exclusively for the purpose of estimating the threshold separation $R_T$, we have carried out a series of calculations using two-layer (Ta+Cl) supercells. We find that the two-layer results not only reproduce the qualitative trends in the site dependence of the adsorption energy, but also give quantitative agreement with the repulsion energies obtained from the nine-layer calculations (see below).

TABLE I. Energetics, work-function change, and structural parameter for the equilibrium geometries of Cl in four adsorption sites on Ta(110) and at a coverage of 1 ML. The intrinsic Ta-Cl bonding energy is defined to be equal to the adsorption energy at 0.5 ML (see text), $E_{\mathrm{bond}}\equiv E_{\mathrm{ad}}(0.5\ \mathrm{ML})$, and is given relative to spin-polarized Cl atoms. The repulsive energy is defined as, $E_{\mathrm{rep}}\equiv E_{\mathrm{ad}}(1\ \mathrm{ML})-E_{\mathrm{ad}}(0.5\ \mathrm{ML})$ (see text). All of the values listed correspond to nine-layer supercell calculations except for those given in parentheses, which correspond to two-layer calculations.

| | Top | Bridge | Hollow | Threefold |
|---|---|---|---|---|
| $E_{\mathrm{bond}}$ (eV) | −4.2 | −4.8 | −5.2 | −5.4 |
| $E_{\mathrm{rep}}$ (eV) | 0.6(0.5) | 0.6(0.6) | 1.0(0.9) | 0.8(0.9) |
| $\Delta\Phi$ (eV) | +0.6 | −0.4 | −1.0 | −1.2 |
| $R_{\perp}$ (Å) | 2.24 | 1.96 | 1.87 | 1.80 |

In the two-layer calculations the Cl atoms were fixed at the minimum-energy geometries obtained from the nine-layer calculations at 1 ML. For all four geometries the calculated adsorption energy is essentially constant up to a coverage of 0.5 ML. At this coverage the Cl-Cl nearest-neighbor distance is equal to the bulk Ta lattice constant, 3.22 Å, for all four adsorption sites. Similarly, we have found that in calculations for the Ta(100) surface (not studied here) the Cl-Cl repulsion is small at a separation of 3.22 Å.[17] Consequently, we have taken this distance as our best estimate of an upper bound for $R_T$, and therefore defined the repulsive energy to be zero at a coverage of 0.5 ML. Table I gives the Cl-Cl repulsion at 1 ML,

$$E_{\mathrm{rep}}=E_{\mathrm{ad}}(1\ \mathrm{ML})-E_{\mathrm{ad}}(0.5\ \mathrm{ML}),$$

obtained using both nine- and two-layer supercells. The agreement between the two sets of calculations is within 0.1 eV/atom for all four geometries, which demonstrates that the two-layer results are sufficiently accurate for the purpose of estimating $R_T$. Perhaps not surprisingly, the Cl-Cl repulsion depends more sensitively on the Cl-Cl separation than an accurate treatment of the Ta substrate. At 1 ML the Cl-Cl nearest neighbor distance is 2.79 Å for all four adsorption geometries. As indicated in Table I, we find that the Cl-Cl repulsion is significant, ranging from 0.6 to 1.0 eV per Cl atom, which is consistent with the experimental observation that the Cl saturation coverage is less than 1 ML.[9]

### B. Ta-Cl bonding energy

Having defined the Cl-Cl repulsion to be zero at a coverage of 0.5 ML the Ta-Cl bonding energy $E_{\mathrm{bond}}$ is equal to the adsorption energy at this coverage,

$$E_{\mathrm{bond}}=E_{\mathrm{ad}}(0.5\ \mathrm{ML}).$$

Table I gives $E_{\mathrm{bond}}$ for all four adsorption sites obtained using nine-layer supercells. These results show that the threefold site is the most stable and not the hollow site as Peralta, Berthier, and Oudar[8] assumed. The intent of these authors was to choose the maximally coordinated site on the bcc(110) surface. While it is true that the hollow site has the

most neighbors, two of the four are located significantly further away than the other two (3.0 versus 2.5 Å) and therefore the hollow site is really twofold coordinated. Thus in practice the threefold site is the maximally coordinated site on bcc(110) surfaces.

### C. Cl overlayer structure

Our *ab initio* calculations have provided a detailed picture of how the Ta-Cl bonding and Cl-Cl repulsion terms vary as a function of adsorption geometry and Cl coverage. We are therefore in a position to make specific predictions regarding the structure of Cl overlayers for coverages other than those directly considered in the calculations. In particular, our prediction for the Cl overlayer structure at the experimentally determined saturation coverage of 0.75 ML (Ref. 9) is shown in Fig. 1(b), where Cl atoms fill two threefold and one hollow site in each unit cell. This geometry was constructed by filling as many of the lowest-energy threefold sites as possible while at the same time minimizing the Cl-Cl repulsion and keeping the coverage fixed at 0.75 ML. We note that the resulting Cl-Cl separations are 3.22, 3.27, and 3.42 Å, equal to or slightly larger than our estimated value of $R_T$. We therefore estimate that the adsorption energy per Cl atom at this coverage is $2/3E_{\text{threefold}}+1/3E_{\text{hollow}}= -5.3$ eV. Increasing the Cl coverage beyond 0.75 ML will inevitably turn on the Cl-Cl repulsion, which may act as a kinetic barrier preventing additional Cl adsorption.

Our proposed 0.75-ML structure also explains the one-dimensional streaking which was observed along $[\bar{1}10]$ in LEED.[9,10] Comparing the surface unit cells for 0.5 and 0.75 ML in Fig. 1, we see that in the 0.5-ML case the Cl atoms occupy only minimum-energy threefold sites. At this coverage there is no repulsion. Between 0.5 and 0.75 ML the length of the unit cell along the [001] direction remains unchanged because the Cl-Cl separation along this direction is equal to $R_T$, and consequently there is little or no cost to fill the next available site along [001]. The streaking results from the increase in the size of the unit cell, which occurs only in the $[\bar{1}10]$ direction. We are thus able to explain the LEED data without the need to invoke vacancy row formation or substrate reconstruction.

### D. Work function and charge density

We next turn our attention to the halogen-induced changes in the work function on bcc transition-metal surfaces. Figure 2 shows the planar-averaged electron density-difference $\Delta\rho$ for 1 ML of Cl in the threeold site and at two different vertical heights $R_\perp$ above the first Ta surface layer of a rigid substrate. The $+$ and $-$ signs in Fig. 2 represent the regions of the Cl-covered surface that are positively or negatively charged relative to the clean surface plus a neutral free-standing Cl layer (note that $+$ refers to a reduction and $-$ to an increase in electron density $\rho$). The *ab initio* results in Fig. 2 strongly suggest that the Cl-induced charge redistribution can be modeled by the sum of three dipole layers, with the corresponding change in the work function given by

$$\Delta\Phi = -\sum_{i=1}^{3} 4\pi e \sigma_i d_i ,$$

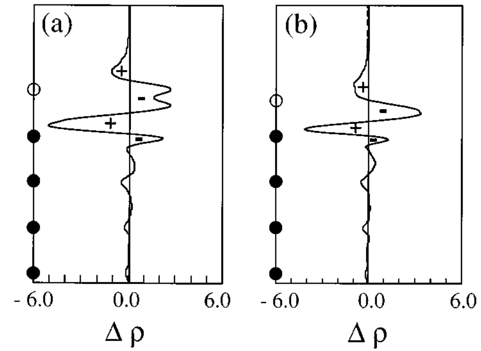


FIG. 2. Cl-induced change in the planar-averaged electron density, $\Delta\rho$ ($10^{-3}$ e/Å$^3$), for 1 ML of Cl at two different vertical heights, $R_\perp$, above the threefold site of Ta(110): (a) $R_\perp$=2.32 Å and $\Delta\Phi=+0.5$ eV; (b) $R_\perp$=1.75 Å and $\Delta\Phi=-1.4$ eV. The vertical positions of the Cl and Ta(110) planes are shown by the empty and filled circles, respectively.

where $\sigma_i$ is the planar charge density and $d_i$ the thickness of an individual dipole layer. We expect that this dipole layer model[4] can be applied generally, and in particular to halogen adsorption on bcc transition-metal surfaces.

The first dipole layer ($i=1$) results from the polarization of the halogen adatom by the field of the metallic surface. It points outwards, and thus contributes to a decrease in the work function upon halogen adsorption. The magnitude increases throughout the halogen series, from F to I, since the atomic polarizability is proportional to the size of the adatom. The second dipole layer ($i=2$) is due to the electronic charge transfer from the metal surface to the adsorbate, which increases the work function. The sign of this contribution is consistent with the relative halogen and transition-metal electronegativities. The third dipole layer ($i=3$) arises from the effect of Smoluchowski smoothing[18] in the metal surface region, and has the same sign as that due to the halogen polarization. The smoothing effect is larger for (110) surfaces than for (100) surfaces, because (110) surfaces have larger interlayer separations and greater planar atomic densities, leading to larger values of $d_3$ and $\sigma_3$, respectively. The overall sign of $\Delta\Phi$ is determined by the competition between the positive contribution from the charge transfer (term 2) and the negative contributions from the adatom polarization (term 1) and Smoluchowski smoothing (term 3). This model is therefore able to explain the work-function decreases for halogen adsorption on (110) surfaces (larger terms 1 and 3) as well as the observed increases for F adsorption (small term 1) and for (100) surfaces (small term 3), all without invoking either Cl subsurface penetration or complex adsorbate phases.

In order to test the accuracy of the dipole layer model against our *ab initio* calculations, we examine the dependence on vertical separation, $R_\perp$, which plays an important role in determining $\Delta\Phi$, since it relates directly to the value of $d_2$. In Fig. 3 we plot the *ab initio* values of $\Delta\Phi$ as a function of $R_\perp$ for 1 ML of Cl in the threefold and hollow adsorption sites on a rigid Ta(110) surface. For both geometries $\Delta\Phi$ is well approximated by a straight line which confirms the validity of the model (linearity in $d_2$), and also indicates that to first order all of the parameters except $d_2$

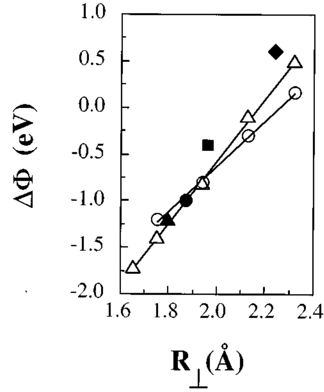


FIG. 3. Cl-induced change in the work function $\Delta\Phi$ as a function of $R_\perp$, for 1 ML of Cl in the threefold (triangles) and hollow (circles) adsorption sites on a rigid Ta(110) substrate. The filled symbols represent the minimum-energy geometries, including the top (diamond) and bridge (square) sites.

can be regarded as independent of $R_\perp$. Thus the positive contribution of the charge-transfer term dominates for large $R_\perp$, resulting in a positive $\Delta\Phi$, while the halogen polarization and Smoluchowski smoothing terms dominate at small $R_\perp$, yielding a negative $\Delta\Phi$. This same trend holds for all four adsorption sites, despite possible differences in the values of the $\sigma_i$ and in the degree of substrate relaxation. This fact is demonstrated by the filled symbols in Fig. 3, corresponding to the four minimum-energy geometries, and providing further evidence of the general applicability of the dipole layer model.

Another test of our proposed overlayer structure at 0.75 ML is the work function, which is generally sensitive to the adsorption geometry (see Table I) when there is charge transfer, as in our case. Due to computational limitations we have not calculated the work function using a supercell for the 0.75-ML structure, but rather from the dipole layer model whose accuracy has been demonstrated above. Our calculations for 0.5 and 1 ML indicate that in this range the work function is nearly independent of coverage for both the threefold and hollow adsorption geometries. Combining this fact with the dipole layer model, we linearly superimpose the dipoles corresponding to the two different adsorption sites, leading to the following estimate:

$$\Delta\Phi(0.75\ \mathrm{ML}) \approx -\sum_{i=1}^{3} 4\pi e[\tfrac{2}{3}\sigma_i(\text{3-fold})d_i(\text{3-fold}) + \tfrac{1}{3}\sigma_i(\text{hollow})d_i(\text{hollow})]$$
$$= \tfrac{2}{3}(-1.2) + \tfrac{1}{3}(-1.0) = -1.1\ \mathrm{eV},$$

where the factors of $\frac{2}{3}$ and $\frac{1}{3}$ represent the fractions of threefold versus hollow sites, and the numerical values in parentheses have been substituted from Table I. Our rough estimate of $\Delta\Phi \approx -1.1$ eV is in qualitative agreement with the experimental value of $-0.75$ eV,[7] lending further support to our proposed overlayer structure.

### E. Electronic structure

In order to obtain insight into the nature of the Ta-Cl bond, we analyzed the surface electronic structure. The energy bands for all four adsorption geometries at 1 ML are plotted in Figs. 4–7. The solid lines are the surface states obtained from the Cl-covered Ta(110) surface calculations, the dotted lines correspond to the bands of a free-standing Cl layer, and the grey pattern indicates the continuum of bulk Ta states. All of the energies are plotted relative to the average bulk electrostatic potential. In all four plots the dispersion of the Cl $3s$ band (approximately 14–19 eV below the Fermi level) for the Cl-covered surface is nearly identical to

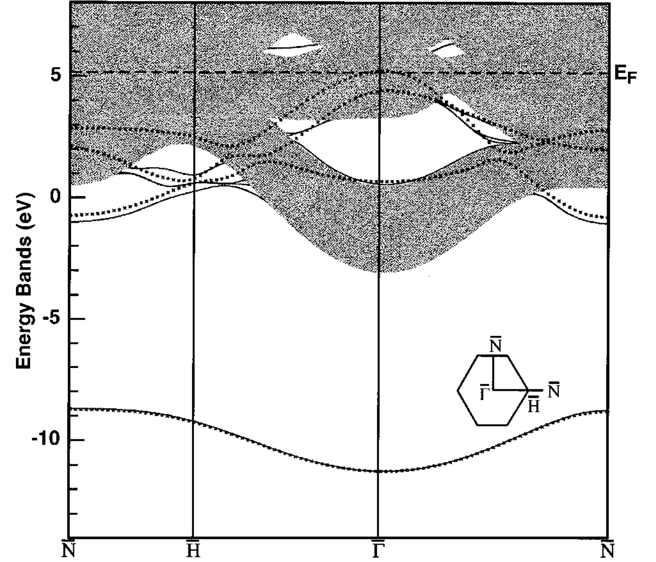


FIG. 4. Energy bands for 1 ML of Cl on Ta(110) in the top site. The solid lines are the surface states obtained from the Cl-covered Ta(110) surface calculations, the dotted lines correspond to the bands of a free-standing Cl layer, and the grey pattern indicates the continuum of bulk Ta states. All of the energies are plotted relative to the average bulk electrostatic potential, and $E_F$ refers to the position of the Fermi level.

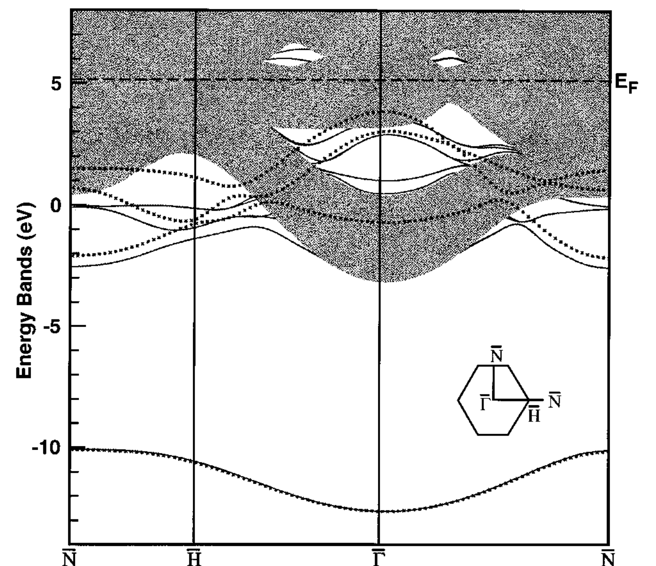


FIG. 5. Energy bands for 1 ML of Cl on Ta(110) in the bridge site.

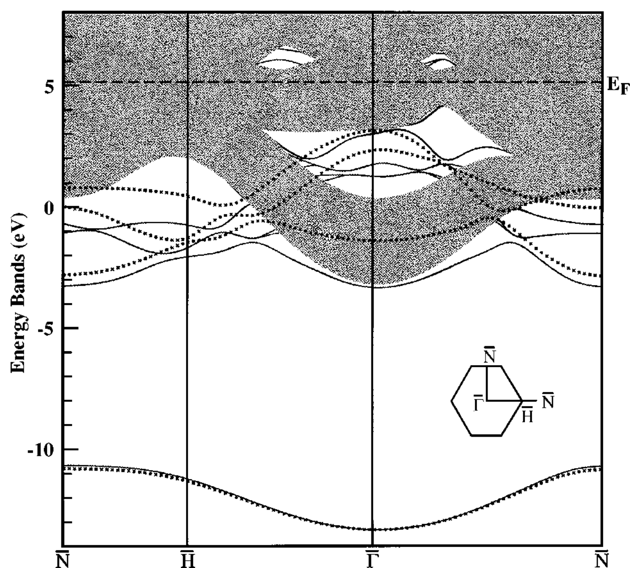


FIG. 6. Energy bands for 1 ML of Cl on Ta(110) in the hollow site.

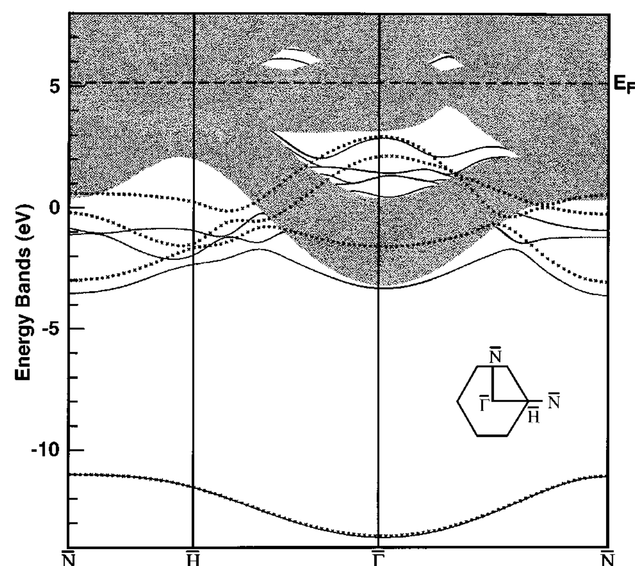


FIG. 7. Energy bands for 1 ML of Cl on Ta(110) in the threefold site.

that of the free-standing Cl layer, which indicates that the Cl $3s$ electrons do not participate in the bonding. In addition, the position of the Cl $3s$ band relative to the Fermi level shifts in direct correspondence to the variations in the work function for the different adsorption geometries (see Table I). Figures 4–7 also exhibit a rich variety of surface states. For example, in Fig. 7 for the threefold site, there is a set of surface states approximately 6–9 eV below the Fermi level along $\bar{N}\rightarrow\bar{H}$. Comparison of these bands with those of the free-standing Cl layer in all four cases shows that the surface states in this energy range are derived from the Cl $3p$ states. All of these Cl $3p$-derived states are occupied which confirms that electronic charge is transfered from the Ta substrate to the Cl overlayer.

We have also carried out a Mulliken population analysis[19] using a full-potential linear muffin-tin orbital method[20] which utilizes a convenient localized basis. This analysis suggests that for all four adsorption sites the dominant contributions to the Ta–Cl bond come from the interaction of Cl $3p$ with Ta $6s$ and $6p$, but surprisingly, much less with Ta $5d$. In hindsight, this result is consistent with the proximity of the Cl-derived surface states to the free-electron-like Ta $sp$ bands, and suggests that Ta looks like a simple metal from the point of view of Cl. This conclusion may apply more generally to highly electronegative adsorbates on transition-metal surfaces and may explain why these adsorbates prefer maximally coordinated sites. The Mulliken analysis also suggests that the Ta-Cl interaction is strongly localized at the surface. This finding is further supported by the nature of the charge-density distribution in Fig. 2, and the fact that the two-layer calculations accurately reproduce the qualitative trends in the adsorption and repulsive energies obtained from the nine-layer calculations. Finally, the validity of our Mulliken analysis is supported by the fact that the integrated bond order for all four geometries reproduces the trend in the *ab initio* adsorption energies.

## IV. SUMMARY

In summary, by carrying out a series of *ab initio* total-energy calculations, we have not only determined a simple Cl overlayer structure on Ta(110) which matches all experimental observations, but we have also provided insight into the nature of the bonding between halogen adsorbates and transition-metal surfaces. Our *ab initio* results exhibit a linear relationship between the work function and the adsorbate-substrate normal separation, providing strong support for a simple dipole layer model. This model is able to explain the unexpected behavior observed in the work function upon halogen adsorption, without invoking the presence of Cl subsurface penetration or complex adsorbate phases. We find that the unusual decrease of the work function results from both a large halogen polarization effect and the effect of Smoluchowski smoothing which is large for (110) surfaces. We believe that the dipole layer model is sufficiently general that it can be widely applied to other systems. We have also explained the one dimensional streaking observed in LEED by means of the geometrical arrangement of adsorption sites and the Cl-Cl mutual repulsion, but without the need to invoke vacancy row formation or substrate relaxation. Finally, we find that the halogen-transition-metal substrate interaction is strongly localized at the surface, and that the substrate looks like a simple metal from the point of view of highly electronegative adsorbates.

## ACKNOWLEDGMENTS

We would like to thank L. H. Yang and C. Mailhiot for numerous helpful discussions, and Jannette Bradley for her assistance in producing the plots of the projected band structures. This work was performed under the auspices of the U. S. Department of Energy by the Lawrence Livermore National Laboratory under Contract No. W-7405-ENG-48.

[1] H. N. Waltenburg and J. T. Yates, Jr., Chem. Rev. **95**, 1589 (1995); H. F. Winters and J. W. Coburn, Surf. Sci. Rep. **14**, 161 (1992).
[2] D. L. Fehrs and R. E. Stickney, Surf. Sci. **17**, 298 (1969).
[3] A. J. Sargood, C. W. Jowett, and B. J. Hopkins, Surf. Sci. **22**, 343 (1970).
[4] C. W. Jowett and B. J. Hopkins, Surf. Sci. **22**, 392 (1970).
[5] F. Bonczek, T. Engel, and E. Bauer, Surf. Sci. **97**, 595 (1980).
[6] J. S. Foord and R. M. Lambert, *Proceedings of ICSS-4 and ECOSS-3*, edited by D. A. Degras and M. Costa (Societe Francaise du Vide, Paris, 1980), Vol. 1, p. 241.
[7] Z. Stott and H. Hughes, Vacuum **126**, 455 (1983).
[8] L. Peralta, Y. Berthier, and J. Oudar, Surf. Sci. **55**, 199 (1976).
[9] Z. Stott and H. Hughes, Vacuum **31**, 487 (1981).
[10] L. A. DeLouise, Surf. Sci. **324**, 233 (1995).
[11] D. F. Klemperer, J. Appl. Phys. **33**, 1532 (1962).
[12] P. Hohenberg and W. Kohn, Phys. Rev. **136**, B864 (1964).
[13] N. Troullier and J. L. Martins, Phys. Rev. B **43**, 1993 (1991).
[14] C. J. Wu, L. H. Yang, J. E. Klepeis, and C. Mailhiot, Phys. Rev. B **52**, 11 784 (1995).
[15] D. M. Ceperley and B. J. Alder, Phys. Rev. Lett. **45**, 566 (1980); J. P. Perdew and A. Zunger, Phys. Rev. B **23**, 5048 (1981).
[16] H. J. Monkhorst and J. D. Pack, Phys. Rev. B **13**, 5188 (1976).
[17] C. J. Wu and L. H. Yang (unpublished).
[18] R. Smoluchowski, Phys. Rev. **60**, 661 (1941).
[19] R. Hoffman, Rev. Mod. Phys. **60**, 601 (1988).
[20] A. K. McMahan, J. E. Klepeis, M. van Schilfgaarde, and M. Methfessel, Phys. Rev. B **50**, 10742 (1994).